# ENGINEERING APPROACHES TO CROSS-SHORE SEDIMENT TRANSPORT PROCESSES

NICHOLAS C. KRAUS

*Coastal Engineering Research Center*
*U.S. Army Engineer Waterways Experiment Station*
*Vicksburg, Mississippi USA*

## 8.1 Introduction

In this chapter we consider beach profile and cross-shore sediment transport processes commonly encountered in coastal engineering applications. Main emphasis is on beach profile change produced by direct wave action, and our assumption will be that longshore transport processes are constant along the profile. This assumption holds best on an open coast far from structures that might produce persistent gradients in longshore currents and sediment transport. For example, impoundment of sediment at a jetty that would otherwise move alongshore and into the inlet or navigation channel causes considerable "gentling" of the beach profile in its vicinity. In this chapter, we avoid such situations.

Until recently most quantitative information on beach profile change and cross-shore transport was obtained in small wave tanks with monochromatic waves of fixed height. As useful as these controlled environments are, *scale mismatches* make both qualitative and quantitative results questionable. By scale mismatch or "scale effects" we refer to an inconsistency such as the wave height and period are greatly reduced in small facilities (typically to on the order of 10 cm and 2 sec) in comparison to the field, but the sand grain size cannot be correspondingly reduced without entering another size classification and different physical or chemical properties. Therefore, small-scale testing should be viewed as a preliminary procedure to gain insight and experience for conducting more expensive large-scale tests and field measurements on profile change and cross-shore sediment transport. The reader is invited to consult Johnson (1949) to find that scaling relations in coastal sediment processes were identified early in the field, and Hughes and Fowler (1990) provides a thorough treatment of movable-bed scale model testing based on the current state of knowledge.

A limited number of large wave tanks exist at present (one each in Germany, Japan, The Netherlands, and the United States) that can be used to study cross-shore sediment transport under *prototype*- or field-scale conditions. Such facilities are on the order of 100 to 200 m long and several meters wide and deep. Wave heights and periods can reach 1 to 2 m and 5 to 10 sec; early configurations of these large tanks allowed generation of only monochromatic waves, but in the past several years random wave generators with reflection compensation (absorption of short-period waves reflected form the beach) have been installed to permit study of cross-shore hydrodynamics and sediment transport processes under random waves. Kraus, Smith, and Sollitt (1992) describe the large-scale *SUPERTANK* laboratory data collection project that used modern instrumentation (as many as 120 channels of data collected at one time!) and wave generator technology to investigate cross-shore hydrodynamic and sediment transport processes.

Field measurement and observation in the coastal zone is most desirable and necessary, but extremely difficult. Difficulties abound, including uncontrollable sea state conditions (random calms and storms), nonhomogeneities in space and time, large area to be covered, corrosion of instruments, problems in mounting instruments, interactions between the instruments, mounts, water, and sediment (for example, instrument-induced fluid vortices and scour), mechanical and electrical cabling problems, and so on. With water motions

and fluid-sediment interaction occurring on many temporal and spatial scales, measurements are often confusing, and we sometimes want to shout "will the real cross-shore sediment transport processes please stand up!" On the other hand, these difficulties are what make our subject so interesting and challenging. At the Field Research Facility of the U.S. Army Corps of Engineers, located in North Carolina on the U.S. Atlantic coast, a 9-year-long continual (weekly) monitoring of the beach profile and incident waves is yielding valuable data on long-term, short-term, and three-dimensional beach morphology change (e.g., Howd and Birkemeier 1987).

Present engineering knowledge of cross-shore transport processes draws heavily on conceptual models that simplify the target problem to a manageable state that is hoped represents the essence of the phenomenon. The engineer should be aware of both the strengths and limitations of these simplifying techniques and models used. Such engineering approaches will be described here. Example calculations for selected topics are presented to show the applications of the material presented here.

## 8.2 Equilibrium Properties of Beach Profiles

Here we consider selected *equilibrium properties* of the beach profile, initially following in part the development given in Larson and Kraus (1989). In the present context, the term "equilibrium" is meant to indicate a situation in which the water level, impressed waves, water temperature, etc., are held constant for sufficiently long time such that the beach profile arrives at a final, stable shape. Thereafter the profile shape does not change further on the meso-scale (order of meters) and greater, even though individual particles are in motion. In other words, in such an equilibrium state the *net* cross-shore transport rate is zero averaged over several wave periods.

In nature, an equilibrium profile shape is seldom observed because the winds, waves, and water level are always changing. The concept is very useful however, in providing a reference for understanding complex transport and morphological processes. In the laboratory, we can well approximate an equilibrium profile, and our discussion will first focus on large tank tests with monochromatic waves reported by Kraus and Larson (1988) and Larson and Kraus (1989). The results will be "ground-truthed" with field data where possible.

Notation for describing beach profile characteristics is given in Figs 8.1a and 8.1b, which respectively illustrate the bar and berm regions of the beach profile (not necessarily corresponding to the same profile and wave conditions).

### A. Longshore Bars

Several hydrodynamic mechanisms have been identified that may produce or maintain a longshore bar. Principle candidate mechanisms are standing waves, infragravity waves, and breaking waves. Here we treat bar formation and movement as produced by breaking waves. Fig. 8.2 shows formation, growth, and movement of a bar created by breaking

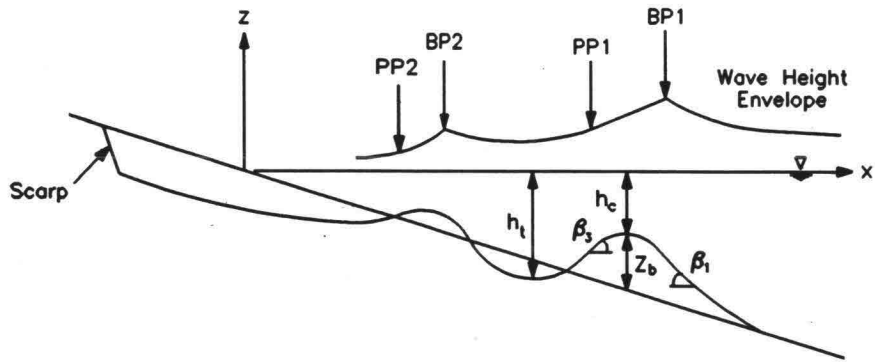


a. Bar properties

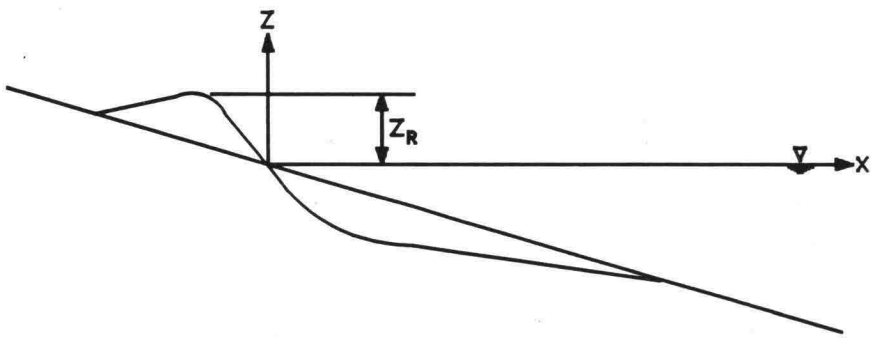


b. Berm properties

Fig. 8.1. Notation for selected bar and berm properties

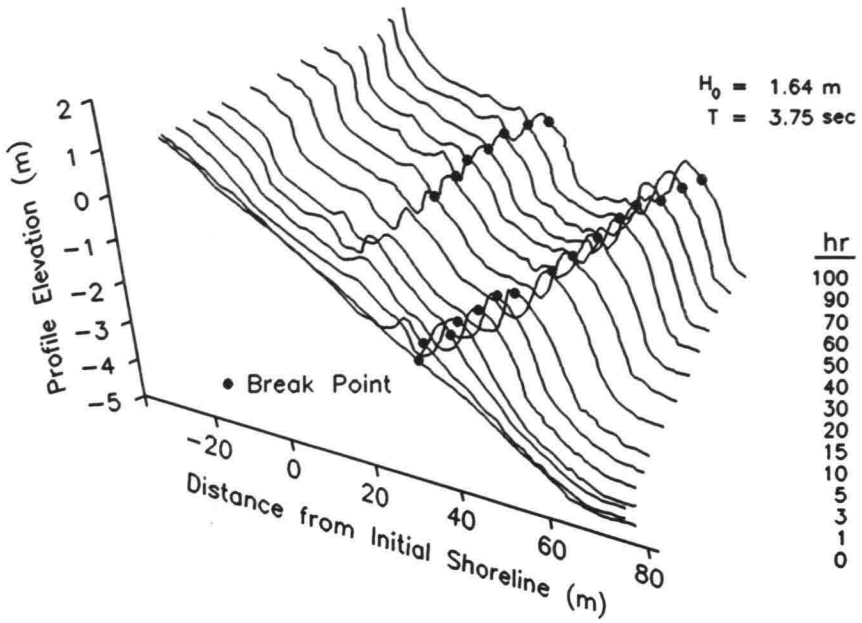


Fig. 8.2. Growth of break-point bar and movement of bar and break point (after Larson and Kraus 1989)

waves in the Corps of Engineers experiments performed by Saville (1957) in a tank 194 m long, 4.6 m wide, and 6.1 m deep. In this test, 0.22-m diameter sand was placed in the form of a 1/15 planar beach, and 1.64-m high deep-water waves of period 3.75 sec (giving a wave steepness of 0.0750) were run for 100 hours. Fig. 8.2 shows that a primary bar formed about 40 m offshore and migrated offshore as the bar and wave interacted. A smaller bar eventually formed nearer to shore by waves that broke again after reforming in the large trough landward of the primary bar. Note that these steep wave eroded the foreshore and produced a scarp.

The break-point bar formed rapidly at first, and thereafter its volume increased more slowly as the profile shape approached equilibrium. Fig. 8.3 shows the growth of bar volume, as calculated with reference to the initial profile for all the Corps of Engineers (CE) tank tests in which a bar formed. The volume grow exponentially to approach an apparent limit under the constant impressed waves. Equilibrium behavior is exhibited by other morphologic features as well, such as berms and surf zone slope.

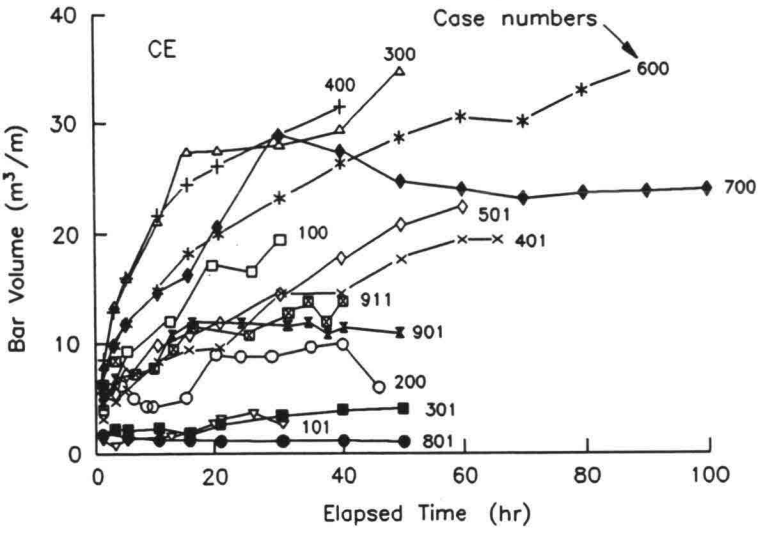


Fig. 8.3. Growth of bar volume (after Larson and Kraus 1989)

The depth at the crest $h_c$ of the equilibrium break-point bars formed in two large wave tank programs (the Corps tests and tests performed in Japan - see Kajima et al. (1983) and Larson and Kraus (1989)) was found to be solely related to the (monochromatic) breaking wave height $H_b$ as

$$h_c = 0.66 H_b \tag{8-1}$$

Sunamura (1989) found the result $h_c = 0.59 H_b$ for small-scale tank tests with movable sand bottoms, giving a coefficient differing little from the 0.66 found for large tanks.

In studies on wave breaking and break-point bars performed during World War II in preparation for beach landing operations, Keulegan (1945, 1948) determined the ratio of bar trough depth $h_t$ to bar crest depth. He found values of $h_t / h_c$ of 1.69 for small-scale laboratory beaches and an average value of 1.65 for field beaches. Shepard (1950) found much smaller $h_t / h_c$ values at Scripps pier, La Jolla, California, with an average value of 1.16 for depth referenced to mean sea level. The smaller value determined by Shepard is expected because the tidal range is relatively large along the Southern California coast (order of 2 m), and the long-period random waves at this Pacific Ocean coast would tend to smooth the profile. The large wave tank analyzed by Larson and Kraus (1989) tests gave

$$\frac{h_t}{h_c} = 2.50\left(\frac{H_o}{L_o}\right)^{0.092} \tag{8-2}$$

by regression analysis.

Equilibrium bar height $Z_b$ in the large tank tests can also be obtained by dimensional regression analysis against potential governing wave and sediment properties... deep-water wave height, $H_o$, wave period $T$, and sediment fall speed, $w$. Forming nondimensional parameters resulted in the equation

$$Z_b = 0.122\left(\frac{H_o}{wT}\right)^{0.59}\left(\frac{H_o}{L_o}\right)^{0.73} \tag{8-3}$$

for bar heights measured from the initial profile ranging from 0.5 to 2.5 m. Note that it is difficult to measure or define bar height in the field because of lack of an unambiguous initial profile shape.

In Eq. 8.3, the quantity $H_o/L_o$ is familiar to us as the deep-water wave steepness. The quantity

$$N_o \triangleq \frac{H_o}{wT} \tag{8-4}$$

is another dimensionless parameter that is found to be very useful for characterizing equilibrium profile properties and is often referred to as the fall time parameter or the Dean number (Dean 1973). It will be discussed below in some detail.

Returning to Fig. 8.3, we have already seen that bars move offshore after being formed in their approach to an equilibrium volume, height, and position offshore. For example, Sallenger, Holman, and Birkemeier (1985) observed an offshore bar crest migration speed of 2.2 m/hr during the initial phase of a large storm. The large wave tank studies gave similar bar speeds. Sunamura (1987) summarized several data sets on time evolution and equilibrium properties of bars formed under breaking waves (The key operative word here is "formed," meaning that the bars were produced starting from an initial profile not in equilibrium with the waves that create and move the bar; the rate of growth of profile change will be high in such a case.) Sunamura obtained the empirical equation

$$\frac{X_B}{L_o} = A_B\left[1 - \exp\left(-\alpha\frac{t}{T}\right)\right] \tag{8-5}$$

for the bar crest horizontal location $X_B$, where $A_B = 1.1 \cdot 10^4 (H_b/gT^2)^2$, the decay coefficient $\alpha = 3.5 \cdot 10^{-8}(H_b/gT^2)^{-1.5}$, $g$ = acceleration due to gravity, and $t$ = time.

As an example, from Eq. 8.5, the speed of a bar crest $C_B$ may be estimated by the equation $C_B = 6.13 \cdot 10^{-5} (gH_b)^{1/2} \exp(-\alpha\, t/T)$. Therefore, the speed of a bar under

5-m breaking waves is on the order of 1.5 m/hr according to this expression. (Note: we assume the bar is created from a non-equilibrium profile shape.)

Eq. 8.5 and the previous example, again demonstrate the approximate exponential behavior of the beach profile in its approach to equilibrium.

The growth of a bar is ultimately limited by the maximum slope the sand grains can maintain without moving under the action of gravity and fluid motion. If this limiting slope is exceeded avalanching will occur, and sand will move down slope and be redistributed to form a more stable, gentler slope and bar shape. In the field, random wave and varying water level exert a smoothing effect on the profile. In the Great Lakes, tidal variations are absent, tending to produce steeper and more well-defined bars than on an ocean coast with a tide. Hands (1976) found that the maximum nearshore bottom slope was less than 10 deg in numerous beach profile surveys performed along Lake Michigan. In the laboratory, monochromatic waves and constant water level produce relatively steep bars that can reach 25-deg slopes on the shoreward side and 18-deg slopes on the seaward side.

In the field and in the laboratory, the shoreward bar slope is almost always steeper than the seaward slope. It may not be uncommon for the shoreward bar slope to reach a critical steepness, then avalanche. Conceptually, for a bar formed at and maintained by breaking waves, the vortex created by breaking and the resultant undertow seem likely explanations for the steep shoreward face.

## B. Berms

In the summer (in the northern hemisphere), lower wave heights move sand shoreward along the beach profile and deposit on the beach face, often to form a wide beach. Similarly, at the end of a storm, when the wave decrease in height while maintaining a long period, the transport direction reverses from offshore to onshore, and material builds up on the foreshore to form a berm. Successive storms are, therefore, usually separated by an interval of onshore transport and berm formation, and this process has become important in engineering practice for estimating storm impacts. In a given year it may happen that several storms with 1- or 2-year frequency occur. The storms would probably not have a cumulative erosional impact on the coast owing to berm build formation inbetween. The *storm recovery* process, which can be very rapid (order of a few days or a week) has been documented by Hayes and Boothroyd (1969), Sonu (1970), Kriebel (1987), and others.

Berm processes are in great need of study. Because berms are formed in the swash zone, at the edge of the runup limit, their location and, probably, many other properties depend on the wave runup height, although beach porosity (related to grain size) and level of the water table must also enter. For the large wave tank experiments, Larson and Kraus (1989) found a fairly clear relation between the maximum subaerial elevation $Z_R$ of the active profile for both bar- and berm-type profiles (Fig. 8.1b), given by

$$\frac{Z_R}{H_o} = 1.47\,\xi_o^{0.79} \tag{8-6}$$

where $\xi_o = \tan\beta\,(H_o / L_o)^{-1/2}$ is the surf-similarity parameter, and $\tan\beta$ was taken as the initial beach profile slope, an approximation for the beach-face slope that was actually changing in these laboratory experiments showing significant erosion and accretion.

The beach-face slope is normally very linear, although the slope is steepest under persistent accretionary wave conditions and gentlest under storm wave conditions (apart from the steep storm scarp if one is formed). Sunamura (1989) has presented separate empirical equations to estimate beach-face slopes in the laboratory and the field. Kriebel, Kraus, and Larson (1991) reanalyzed the field data of Sunamura and obtained the following expression for the beach-face slope $m_f$ as

$$m_f = 0.15\left(\frac{wT}{H_b}\right)^{1/2} \tag{8-7}$$

where the quantity in parentheses is the inverse of the Dean number (Eq. 8.4) evaluated at breaking, denoted as $N_b$. It should be pointed out that there is wide scatter in the data, as seen in Fig. 8.4, and Eq. 8.7 represents a trend for beach face slopes ranging from about 0.04 to 0.2 on the average. As the wave height increases, making $N_b$ larger, the beach face slope decreases, as found in nature.

## 8.3 Equilibrium Beach Profile ($x^{2/3}$)

It was demonstrated in the previous section that the beach profile will approach a certain shape that may include bars and berms if the wave and water level remain unchanged. If we become more abstract in characterizing the profile, the berms and bars may be considered as small perturbations on an idealized shape that has a linear beach-face slope joining a concave curve that gradually becomes more gently sloped with distance offshore. Bruun (1954) and later Dean (1976, 1977) have shown that many ocean beach profiles exhibit a concave shape such that the depth varies as the two-thirds power of distance offshore along their submerged portions. The concept of such a simple yet realistic idealized shape has proven to be very useful in engineering studies involving changes in the beach profile. The most comprehensive theory and application of beach profile concepts has been advanced by Dean (1976, 1977, 1984, 1987, 1991) and his students and colleagues, and we will review some of those developments.

Dean (1977) assumed that the equilibrium profile is associated with uniform energy dissipation per unit volume in the surf zone as

$$\frac{1}{h}\frac{dF}{dx} = D_e \tag{8-8}$$

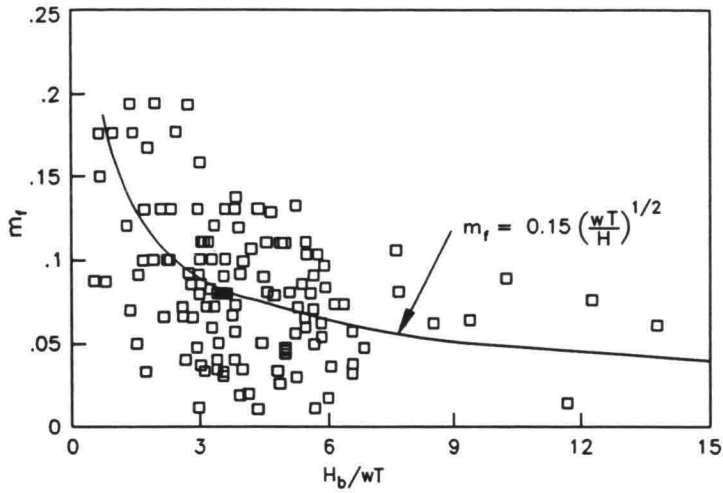


Fig. 8.4. Behavior of beach-face slope
(from Kriebel et al. 1991)

where $h$ = water depth at a distance $x$ from the shoreline, $F$ = wave energy flux in shallow water, and $D_e$ = constant energy dissipation per unit water volume of breaking waves on a profile in equilibrium shape. The wave energy flux in shallow water is given by

$$F = \frac{1}{8}\rho g H^2 \sqrt{gh} \tag{8-9}$$

where $\rho$ = water density, and $H$ = local wave height. We assume that the shallow-water wave height is depth-limited as

$$H = \gamma h \tag{8-10}$$

where $\gamma$ = breaker index ($\gamma \simeq 0.78 \sim 1$), as might be valid for high steepness waves breaking on a gently sloping beach, i.e., spilling breakers. (However, we apply Eq. 8.10 with impunity for any type of surf zone condition at the present time!) One then has

$$F = \frac{1}{8}\rho g^{3/2}\gamma^2 h^{5/2} \tag{8-11}$$

Substituting Eq. 8.11 into Eq. 8.8 and integrating under the condition $h = 0$ at $x = 0$ gives

$$h = A x^{2/3} \tag{8-12}$$

where

$$A = \left(\frac{24\, D_*}{5\rho g^{3/2}\gamma^2}\right)^{2/3} \tag{8-13}$$

Eq. 8.12 is the equilibrium profile in most engineering discussions of beach shape.

The "$A$" parameter, sometimes called the profile shape parameter, controls the steepness of the profile, and the power 2/3 produces the desired concavity. The most widely used design information available for determining $A$ is that given the Masters degree thesis of Moore (1982), in which $A$ is related graphically to the median grain size, $d_{50}$. Moore's development rests on analysis of 40 beach profiles encompassing grain size diameters ranging from 0.1 mm to 30 cm (the latter from a profile published by Zenkovich (1967) for a boulder beach on the coast of Eastern Kamchatka, of the former Soviet Union, facing the northern Pacific Ocean), and thus the simple equilibrium ($x^{-2/3}$) profile shape has substantial reliability. The following equations provide an analytic description of Moore's curve based on visual fit (Hanson and Kraus 1989):

$$\begin{aligned} A &= 0.41(d_{50})^{0.94} \quad , \quad d_{50} < 0.4 \\ A &= 0.23(d_{50})^{0.32} \quad , \quad 0.4 \le d_{50} < 10.0 \end{aligned} \tag{8-14}$$

$$\begin{aligned} A &= 0.23(d_{50})^{0.28} \quad , \quad 10.0 \le d_{50} < 40.0 \\ A &= 0.46(d_{50})^{0.11} \quad , \quad 40.0 \le d_{50} \end{aligned}$$

Dean (1987) gave an alternate empirically-derived representation for $A$ by expressing it in terms of the sediment fall speed, $w$. Kriebel, Kraus, and Larson (1991) obtained an expression for $A$ as a function of the fall speed by using a simple model sediment suspension in the surf zone proposed by Kraus, Larson, and Kriebel (1991), in which the

concentration of suspended particles $\beta$ is proportional to the energy dissipation per unit volume, $D_e$. To obtain this expression, we note that the work $W$ required to maintain grains of density $\rho_s$ in suspension is given by

$$W = \beta (s - 1) \rho g w \tag{8-15}$$

where $s = \rho_s / \rho$. If a fraction of the equilibrium energy dissipation $\epsilon$ is expended to maintain the concentration, we have

$$\epsilon D_e = \beta (s - 1) \rho g w \tag{8-16}$$

Solving Eq. 8.16 for $D_e$ and substituting this into Eq. 8.13 gives

$$A = \left[ \frac{24 \beta (s - 1)}{5 \epsilon \gamma^2} \right]^{2/3} \left( \frac{w^2}{g} \right)^{1/3} \tag{8-17}$$

This expression has the same functional dependence, $(w^2/g)^{1/3}$, as the profile shape derived by Bowen (1980) based on Bagnold's (1963) energetics-based transport formula for suspended sediment transport. By comparison of the functional dependence of Eq. 8.17 on $w$ and Moore's (1982) data, the relation between $A$ and $w$ is found to be

$$A = 2.25 \left( \frac{w^2}{g} \right)^{1/3} \tag{8-18}$$

This expression is appropriate for a water temperature of about 20° C for sediment sizes typical of sand beaches where the fall speed is in the range of 1 to 10 cm/sec. In this range, Eq. 8.18 agrees reasonable well with the empirical relationship between $A$ and $w$ given by Dean (1987). Fig. 8.5 illustrates the dependence of the $A$-parameter on sediment grain size and fall speed.

As an example, we compute and compare predictions for the shape-parameter $A$ obtained from Eqs. 8.14 and 8.18 for a 0.30-mm diameter sand beach. By Eq. 8.14, $A = 0.41\ (0.30)^{0.94} = 0.13\ \text{m}^{1/3}$. To use Eq. 8.18 determine the fall speed from Fig. 8.5 to give $w = 0.039$ m/sec. We then find $A = 2.25\ (0.039^2/9.81)^{1/3} = 0.12\ \text{m}^{1/3}$. The values are remarkably close considering the visual fit used to arrive at Eq. 8.14 and evaluation of the fall speed from grain diameter by an independent empirical relation.

### 8.4 Equilibrium Profile with Sloping Beach Face

A mathematical annoyance with the expression $h = Ax^{2/3}$ is that the slope given by $dh/dx = 2/3\, A x^{-1/3}$ becomes infinite at the shoreline, $x = 0$. The beach face is not a vertical wall, but, instead typically has a linear slope, as previously discussed.

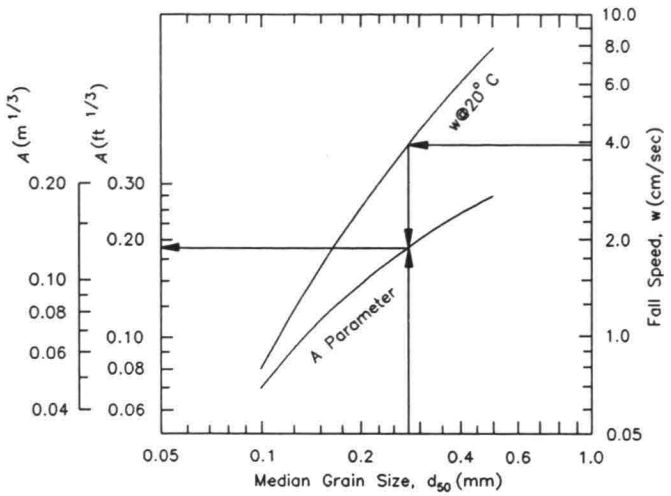


Fig. 8.5. Dependence of $A$ on sediment grain size and fall speed (Kriebel et al. 1991)

For practical applications, the equilibrium profile may be adopted for the surf zone and replaced by a linear beach face of specified slope $m_f$ at the depth $h_T$ where the two curves become tangent. The depth $h_T$ is given by

$$h_T = \frac{4}{9}\frac{A^3}{m_f^2} \tag{8-19}$$

By substituting representative values for $A$ and $m_f$ in the equation, it is found that the depth joining the two profiles is quite small for a fine-grained sandy beach.

By generalizing the simple spilling breaking wave model $H = \gamma h$, is possible to derive a more realistic equilibrium profile shape, one that has a plane beach-face slope joining and $x^{2/3}$ concave slope (Larson and Kraus 1989), and we sketch the derivation here. The wave energy dissipation per unit water volume is assumed to be given by the wave decay model of Dally, Dean, and Dalrymple (1985), which is

$$D = \frac{\kappa}{h^2}(F - F_s) \tag{8-20}$$

In words, this expression gives the energy dissipation as the difference between the energy flux $F$ of a broken wave and the flux of a wave that is *stable*, i.e., no longer breaking

because the wave height can be maintained at the water depth it is in. This height, achieved after breaking, was found to be given by $H = \Gamma h$, where $0.35 < \Gamma < 0.475$. The stable wave energy flux is then

$$F_s = \frac{1}{8}\rho g^{3/2}\Gamma^2 h^{5/2} \tag{8-21}$$

in analogy with Eq. 8.11. The quantity $\kappa$ expresses the steepness at which the wave height decays, and has the range $0.1 < \kappa < 0.275$. Best overall values as found by Dally et al. are $\kappa = 0.15$ and $\Gamma = 0.4$. For a beach in equilibrium, Eq. 8.20 can be solved to find the breaker height at any depth as

$$H = \left(\Gamma^2 h^2 + \frac{8D_e}{\rho g^{3/2}\kappa} h^{3/2}\right)^{1/2} \tag{8-22}$$

By substituting this equation for the wave height into Eq. 8.8, $D_e = 1/h\ dF/dx$, and integrating over the surf zone with the boundary condition $h = 0$ at $x = 0$, an *equilibrium profile shape* is obtained as

$$x = \frac{2}{\kappa}h + \frac{5\rho g^{3/2}\Gamma^2}{24D_e} h^{3/2} \tag{8-23}$$

which can be rewritten in the form,

$$x = \frac{h}{m_*} + \left(\frac{h}{A_*}\right)^{3/2} \tag{8-24}$$

where

$$m_* \triangleq \frac{\kappa}{2} \tag{8-25}$$

is identified as the beach-face slope and

$$A_* \triangleq \left(\frac{24D_e}{5\rho g^{3/2}\Gamma^2}\right)^{2/3} \tag{8-26}$$

has the same form as Eq. 8.13 derived by Dean (1977) for the spilling wave assumption, but with the stable wave height parameter $\Gamma$ replacing the breaker index $\gamma$. Because $\Gamma \approx 1/2\gamma$, we have $A_* \approx 2^{4/3} A = 2.52\, A$. No re-analysis of Moore's (1982) data set has yet

been done to quantify the new parameter $A$. as a function of grain size and wave conditions.

## 8.5 Applications of Equilibrium Beach Profiles

In the previous sections it was shown that if the waves and water level are constant, the beach profile will adjust to reach a new shape that is in equilibrium with the hydrodynamic conditions in the surf zone. Although bars and berms may form as part of the equilibrium shape, most beach profiles on an open coast have a linear beach face that joins to a concave profile offshore. If we assume that bars and berms are perturbations on this basic equilibrium shape, then in a broad (macro-scale) perspective we can consider and operate with the idealized equilibrium shape that was shown to be a function of the median grain size or fall speed and the wave energy dissipation.

If we accept the equilibrium profile concept and assume that beach erosion and accretion occur such that the profile shape remains intact, then useful results can be derived. The development rests on only two assumptions; (1) the profile moves in parallel to itself or relative to a new water level such that the shape is preserved, and (2) sand volume is conserved. Both cross-shore (beach profile change) modeling and longshore or shoreline change modeling rest on these two principles. The Bruun Rule describing profile recession and beach erosion in response to sea level rise, discussed in Chapter 2, is an application that applies these principles over geologic time scales.

Once equilibrium profile forms are established, analytical solutions describing the equilibrium response to a water level rise, such as storm surge, may be obtained. The phrase "equilibrium response" refers to the final position of the profile if sufficiently long time is allowed to pass; as such, it represents a potential maximum response of the profile.

As one of the earliest applications, Dean (1976) [see also, Dean and Maurmeyer (1983) and Dean (1991)] considered the "square-berm" profile (see Fig. 8.6 for notation) given by the simple form $h = Ax^{2/3}$, and, by equating the eroded and deposited sand volumes, obtained a transcendental equation for the equilibrium berm recession $R_\infty$ ,

$$R_\infty = \frac{x_b S}{B} - \frac{3}{5}\frac{h_b x_b}{B}\left[1 - \left(1 - \frac{R_\infty}{x_b}\right)^{5/3}\right] \tag{8-27}$$

in which $x_b$ = depth of the predominant breaking waves, $S$ = surge level (water elevation rise), $B$ = elevation of the berm from the still-water level, and $h_b$ = water depth at breaking.

If we assume that the horizontal recession, $R_\infty$ is small compared to the width of the surf zone, then Eq. 8.27 reduces to

$$\frac{R_\infty}{x_b} = \frac{S}{B + h_b} \tag{8-28}$$

which has the same form as the Bruun Rule. By carrying out the solution with slightly different geometry, simpler expressions than Eq. 8.27 for the equilibrium profile response can be obtained (Kriebel, Kraus, and Larson 1991).

### A. Square-Berm Profile

The profile configuration for this situation is shown in Fig. 8.6. The solution for the equilibrium beach recession, $R_\infty$, is obtained by shifting the profile upward by an amount $S$ corresponding to the surge, and then landward by an amount $R_\infty$ until the volume eroded from the beach face, $V_1 + V_2$, equals the volume deposited offshore, $V_6 + V_7$. The solution procedure (geometry) differs from that of Dean (1976) leading to Eq. 8.27 in that Dean truncated the profile offshore at the new positions of the breaking depth, whereas a ramp of sand (volume $V_7$) is assumed here between the original and new positions of the breaking depths. (The ramp slightly deviates from the true equilibrium profile principle.)

With this geometry specified, the balance of volumes is simplified if the water volume, $V_3 + V_4 + V_5$ is also included, such that

$$V_1 + (V_2 + V_3 + V_4) + V_5 = V_3 + (V_4 + V_5 + V_6 + V_7)$$

Terms enclosed by parentheses could, in principle, be evaluated by integration of the $Ax^{2/3}$ profile across the surf zone. However, because the profile shape is identical before and after the water level rise, contributions from these terms cancel, eliminating the necessity for the integration.

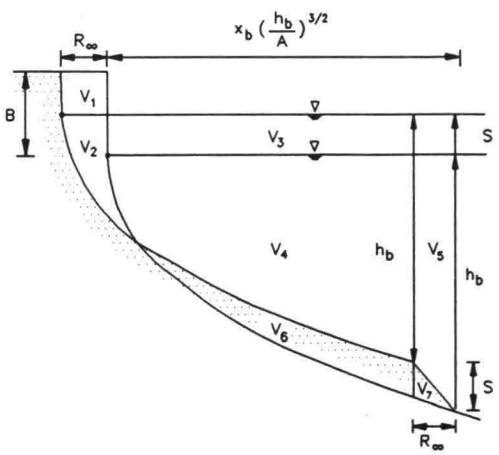


Fig. 8.6. Square-berm profile definition sketch

By the above arguments, conservation of sand requires

$$V_1 + V_5 = V_3$$

and expression of the volumes in terms of the geometry leads to

$$R_\infty = \frac{x_b S}{B + h_b - \frac{S}{2}} \tag{8-29}$$

where

$$x_b = \left(\frac{h_b}{A}\right)^{3/2} \tag{8-30}$$

Eq. 8.29 is similar in form to the Bruun Rule and reduces to it if the rise in water level is small. Under this condition, the solution is equivalent to that of Dean, Eq. 8.27, (rigorous maintenance of equilibrium profile shape) because the volume in the ramp is small. As $S$ increases, Eq. 8.29 predicts somewhat more recession than the Dean expression, perhaps as much as by 10 ~ 20 percent.

### B. Equilibrium Response with Dunes

On many beaches dunes are maintained or constructed for hurricane and storm protection. The equilibrium profile approach can also be applied to idealized situations with high dunes to determine the maximum potential response to a surge. Here we consider a dune connected to a beach with a linear slope on the foreshore.

For a beach backed by a dune with no backshore, Fig. 8.7a, the simplest solution is obtained under the assumption that the water level does not rise above the berm height $B$, and that the entire dune face of height $D$ erodes uniformly, perhaps by collapsing and avalanching. The equation describing the retreat of the dune cost, $R_D$, is

$$R_D = \frac{\left(x_b - \frac{h_b}{m_f}\right) S}{B + D + h_b - \frac{S}{2}} \tag{8-31}$$

in which $m_f$ is the slope of the foreshore. If $m_f \rightarrow \infty$ (vertical wall of sand at the shoreline) and $D = 0$ (no dune), the solution of the previous example is recovered.

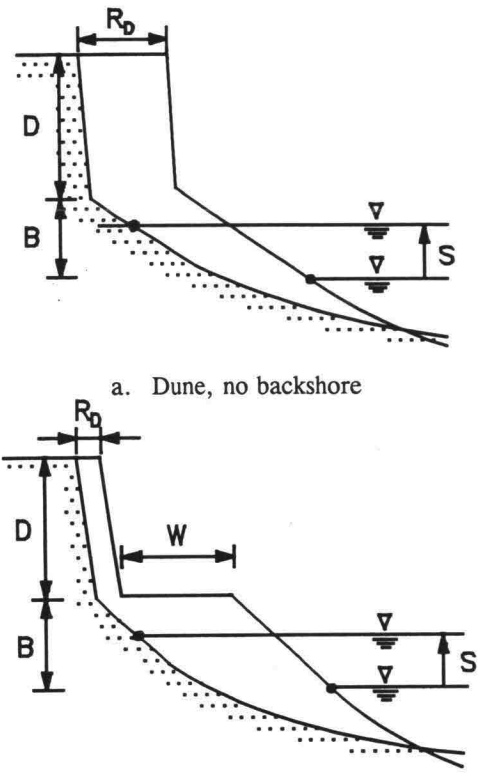


Fig. 8.7. Notation for selected bar and berm properties

If we eliminate the dune, then Eq. 8.31 predicts less erosion (interpreting $R_D$ as $R_\infty$), than the simple equilibrium profile without a plane foreshore (Eq. 8.29). This prediction is in agreement with the findings Kriebel and Dean (1985) and others that beach face slopes (for a given offshore profile) have a greater erosion potential than beaches with milder beach face slopes.

Returning to Fig. 8.7b, if the beach profile is backed by a dune and has a wide backshore of width ($W$), the expression for the recession of the dune becomes

$$R = \frac{\left(x_b - \frac{h_b}{m_f}\right)S}{B + D + h_b - \frac{S}{2}} - \frac{\left(B + h_b - \frac{S}{2}\right)W}{B + D + h_b - \frac{S}{2}} \tag{8-32}$$

For such a beach with plentiful sand supply in the back shore, both the height of the dune and the width of the backshore are beneficial in limiting the retreat of the dune face.

## 8.6 Depth of Closure

We conceptualize that a beach profile responds to wave action between two limits, one limit on the landward side where the wave runup ends and the other limit in deeper water where the waves can no longer produce a measurable change in depth. This latter limit, the minimum water depth at which no change (as measured by engineering means) occurs, is called the *depth of closure*. The depth of closure is not the location where sediment ceases to move, but that location of minimum depth where profile surveys before and after a period of wave action, a storm perhaps, lie on top of one another.

The closure depth enters in a number of applications such as placement of mounds of dredged material to reduce wave action, beach fill, placement of ocean outfalls, and sediment budget calculations. On further inspection of the concept, we realize that the depth of closure is time dependent, that is, dependent upon the transporting capacity of the particular incident waves. For example, we expect the average depth of closure for the summer to be less than that in winter. Similarly, the "storm of the decade" will alter the profile elevation to a much greater depth than occurs during a typical storm season. This time element was recognized by Hallermeier (1979, 1981, 1983), and, in this section, we review selected elements from his work on this subject. His development is more comprehensive than our treatment will represent, and the reader is urged to read the relevant papers.

Active beach profile change is an indication of the seaward extent of the littoral zone. This limiting depth is a function of the wave height, wave period, and sediment size and composition, and it is most reliably determined by reference to repetitive profile surveys and bathymetry maps for the site of a neighboring site that experiences the same wave climate. If adequate profile data do not exist, an analytic method introduced by Hallermeier can be used to estimate the limiting depth. Hallermeier defined an annual seaward limiting depth $h_{sa}$ of the littoral zone as,

$$\frac{h_{sa}}{H_o} = 2.28 - 10.9\frac{H_o}{L_o} \tag{8-33}$$

where $H_o$ = significant deep-water wave height exceeded 12 hr per year, and $L_o = gT/2\pi$ is the deep-water wavelength of the significant waves of height $H_o$ and period $T$. The

second term in Eq. 8.33 is a steepness correction; the leading-order term indicates that $h_{sa} \simeq 2H_o$. Eq. 8.33 is specific to quartz sand and is derived form a more general expression. Hallermeier based his development leading to Eq. 8.33 and similar expressions on laboratory profile change verified with field data from the Pacific Ocean and Gulf of Mexico. Birkemeier (1985) tested Eq. 8.33 with high-quality data from the Coastal Engineering Research Center's Field Research Facility at Duck, North Carolina, and found that is held if the empirical coefficients were adjusted slightly for that site to give $h_{sa}/H_o = 1.75 - 9.2(H_o/L_o)$, thereby validating the basic functional dependence of the equation. Fig. 8.8 shows some of the profile survey data used in the analysis.

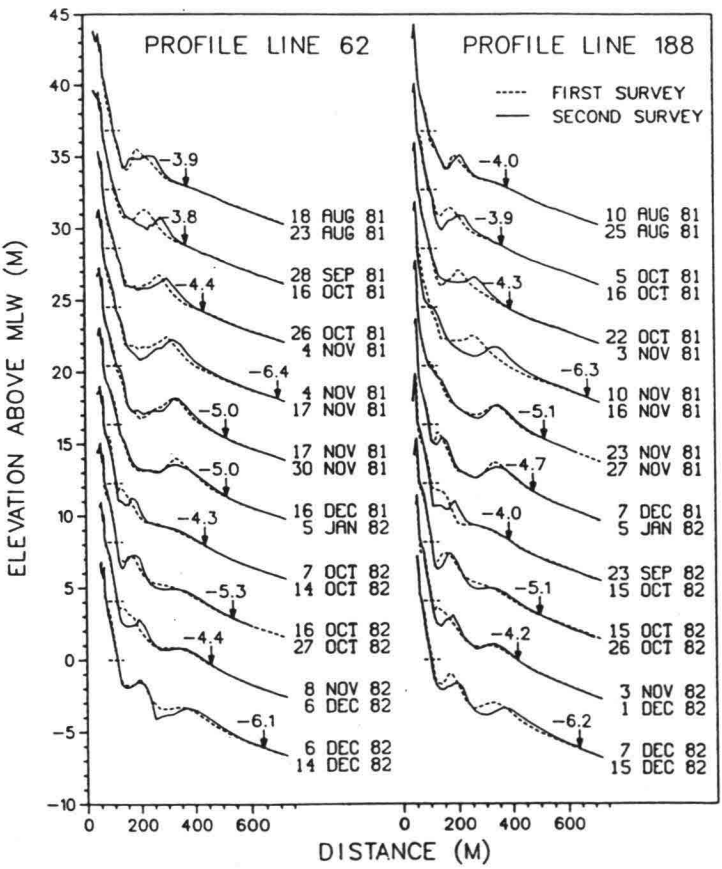


Fig. 8.8. Profile survey data from the Corps' Field Research Facility (Birkemeier 1985)

In a different approach to determining the closure depth, Kraus and Harikai (1983) plotted the standard deviation of depth against average depth, as shown in Fig. 8.9, for eight wide-area bathymetric surveys made on a Pacific Ocean beach in Japan. The curve is a hand-drawn envelope encompassing the majority of data points. The figure indicates that the standard deviation in depth at the site decreases markedly at a mean depth of about 6 m, after which it becomes effectively constant. The non-zero tail in standard deviation is probably an artifact of the accuracy limit of a fathometer survey.

In engineering projects, the depth of closure is best determined through repeated accurate profile surveys, such as performed with a sled. If such data are not available, Eq. 8.33 has been found to give a reasonable estimate of the depth of closure in several applications where ground truthing survey data were available.

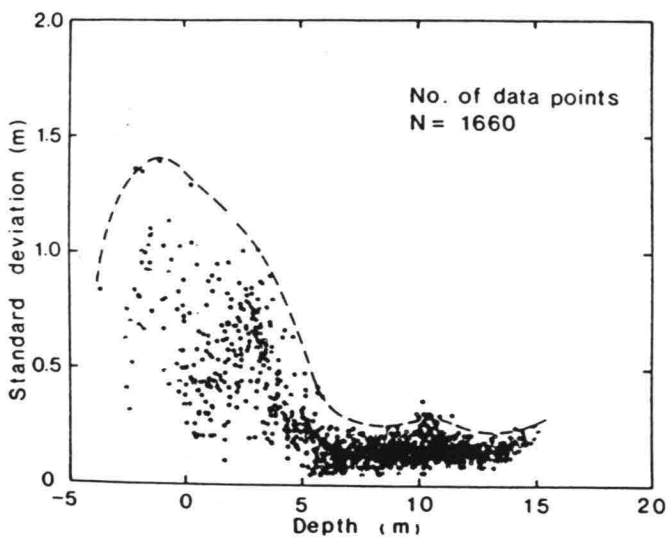


Fig. 8.9. Standard deviation of depth versus average depth for several wide-area surveys (after Kraus and Harikai 1983)

## 8.7 Erosion and Accretion Predictors

In this section, we describe some of the simple techniques that have been found capable of predicting whether a beach will erode or accrete by cross-shore transport processes. Chapter 7, mathematical modeling of beach change will discuss more quantitative approaches.

It is well known that steep winter storm waves and hurricanes tend to remove material from the beach face and deposit it offshore as a bar, whereas summer swell and swell generated during the decay of a storm or hurricane tend to build the berm and widen the beach. Early small-scale wave tank studies with sand beaches indeed found that wave steepness was an important factor. Such work was summarized by Johnson (1949) in an influential paper on scale modeling. Johnson stated that small-scale laboratory fine sand beaches eroded if the deep-water wave steepness exceeded 0.025, but cautioned that scale effects might alter this result. Later, Saville (1957) showed that a beach in a large wave tank could erode if the wave steepness was a tenth of 0.025. Shortly after, Iwagaki and Noda (1962) demonstrated on the basis of small-scale laboratory data, that the parameter $H_o / d$, where $d$ is a representative grain size, provided improved predictive capability if used together with the wave steepness, $H_o / L_o$.

After that time there have been numerous studies of erosion and accretion predictors, many of which are summarized in Larson and Kraus (1989) and Kraus, Larson, and Kriebal (1991). We will review some results from the latter paper in the remainder of this section.

The subject of beach erosion and accretion prediction was greatly stimulated by a 1973 paper of Dean, who derived a predictive criterion from a simple quantitative model of sand particle motion produced by a breaking wave. Suppose that under a breaking wave of height $H_b$, a sand particle is lifted to some elevation $z$ in the water column that is a fraction $\beta$ of the wave height;

$$z = \beta H_b \qquad (*)$$

where $\beta$ is less that but on the order unity. The time $t$ required for the particle to settle to the bottom depends on its fall speed, $w$, as

$$t = \frac{z}{w} \qquad (**)$$

Under the somewhat over-simplified assumption that the horizontal water motion is uniform over depth, if the *fall time* $t$ is less than half the wave period, $T/2$, net onshore water motion under the wave crest would carry the sand particle onshore, whereas if $t > T/2$ (but less than $T$), the particle will move offshore under the wave trough. Combining (*) and (**) to eliminate $t$ we obtain

$$\frac{2\beta H_b}{wT} < 1 \quad , \quad \textit{onshore motion}$$

$$\frac{2\beta H_b}{wT} > 1 \quad , \quad \textit{offshore motion} \tag{8-34}$$

Dean also expressed these conditions as

$$\frac{H_b}{L_o} > \frac{\pi w}{\beta g T} \quad , \quad \textit{onshore motion}$$

$$\frac{H_b}{L_o} > \frac{\pi w}{\beta g T} \quad , \quad \textit{offshore motion} \tag{8-35}$$

The condition expressing onshore motion signifies a summer or accretionary beach profile, and the condition expressing offshore motion signifies a winter or erosional profile. By replacing $H_b$ by $H_o$ and examining small-scale tank data and limited large-tank data of Saville, Dean obtained the criterion

$$\frac{H_o}{L_o} = 1.7 \frac{\pi w}{g T} \qquad (\textit{small scale}!) \tag{8-36}$$

In general, rather than express criteria for predicting erosion or accretion as two equations, such as Eqs. 8.35 or 8.36, we use the equation such as Fig. 8.36 to define a *separation line* between the two regions.

In our discussion, four nondimensional parameters have appeared, to which we now will give symbols to simplify notation and add one parameter to give five basic parameters:

$$D_o \triangleq \frac{H_o}{d} \tag{8.37a}$$

$$F_o \triangleq \frac{w}{(gH_o)^{1/2}} \tag{8.37b}$$

$$G_o = \frac{\pi w}{gT} \tag{8.37c}$$

$$N_o = \frac{H_o}{wT} \tag{8.37d}$$

$$S_o = \frac{H_o}{L_o} \tag{8.37e}$$

The quantity $D_o$ is the inverse of a nondimensional grain size and in some sense expresses the relative strength of a wave to move sediment grains of diameter $d$. The quantity $F_o$ is a Froude-type number expressing the relative strength of the ease of motion of the wave. $G_o$ is in a sense a derived quantity relating $F_o$ and $N_o$. The parameter $N_o$ is called variously as the fall-time parameter, fall speed parameter, and Dean number. Of course, $S_o$ is the wave steepness in deep water.

Beach erosion and accretion (by cross-shore transport) has been classified with parameters other than these and in combination with the five above. One such parameter is the average beach slope, and Sunamura and Horikawa (1974) and Sunamura (1980) have given a predictive criterion that is widely used. The position taken here is that through the equilibrium assumption, the grain size, or sediment full speed should account for the average beach slope.

The capability of the five nondimensional parameters to predict beach erosion and accretion was examined in detail by Kraus, Larson, and Kriebel (1991) by use of a large-wave tank data set containing 32 erosion and accretion events and a field data set containing 99 events. They examined the parameters individually or in pairs, and we show representative results here.

Fig. 8.10 plots the large-wave tank (LWT) erosion and accretion data on the $S_o$ - $N_o$ plane originally considered by Larson and Kraus (1989). The diagonal line separates the filled symbols (erosion) on the right and open symbols (accretion) and is described by $S_o = 0.00070\, N_o^3$ which holds for monochromatic waves in large wave tanks. It was found that this equation separated most of the field events if *mean* wave height was used in $S_o$ and $N_o$. However, in engineering studies *significant* deep-water wave height is usually available. The field data set is plotted in Fig. 8.11 using significant wave height, and a reasonable separation of erosion and accretion events is obtained with the equation

$$S_o = 0.00027\, N_o^3 \qquad (\textit{signif. height}) \tag{8-38}$$

The different symbols (filled → erosion: open → accretion) pertain to different beaches around the world. It is noted that the simple criterion

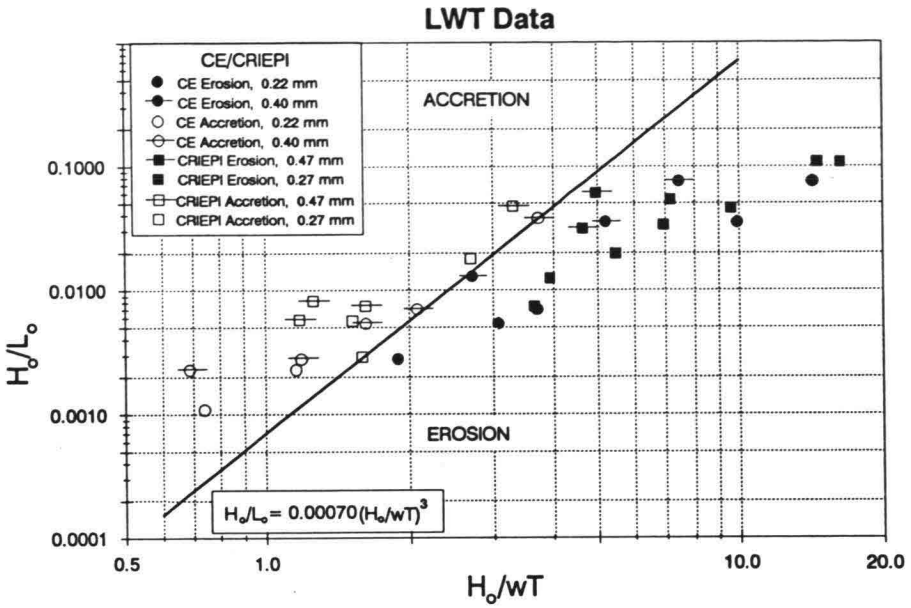


Fig. 8.10. LWT data plotted on the $S_o$ - $N_o$ plan (Kraus et al. 1991)

$$N_o = 3.2 \tag{8-39}$$

also separates most events.

In Fig. 8.11 the dashed lines were developed by assigning a 10% variability in $H_o$, $T$ and $w$. Inspection of the competence of each diagonal line to separate erosion and accretion events leads to the following equations and qualitative interpretation:

If $S_o > 0.00014\ N_o^3$, then ACCRETION is highly probable.

If $S_o > 0.00027\ N_o^3$, then ACCRETION is probable.

If $S_o \leq 0.00027\ N_o^3$, then EROSION is probable.

If $S_o < 0.00054\ N_o^3$, then EROSION is highly probable.

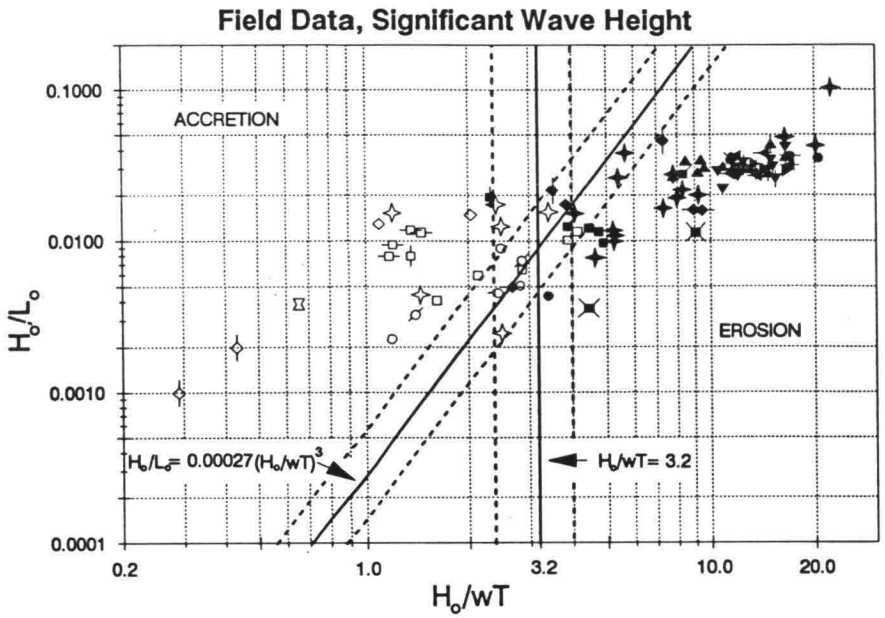


Fig. 8.11. Field data plotted on the $S_o$ - $N_o$ plane (significant wave height)

and (8.40)

If $N_o < 2.4$, then ACCRETION is highly probable.

If $N_o < 3.2$, then ACCRETION is probable.

If $N_o \geq 3.2$, then EROSION is probable.

If $N_o > 4.0$, then EROSION is highly probable.

A PC program called "ON_OFF" is available that implements Eqs. 8.40 in an interactive environment.

We consider a few more examples examining the competence of simple erosion and accretion predictors. Fig. 8.12 gives a plot of the LWT data on the $S_o$ - $G_o$ plane, in which line **A** corresponds to the original criterion of Dean (1973) based on data from small tanks, line **B** is a line parallel to **A** with a coefficient modified to fit the LWT data, and line **C** is a rotated line given by $S_o \propto G_o^{2/3}$ that somewhat better separates the data. The small-scale laboratory results provide the same dependencies, with only an adjustment in the magnitude of the empirical coefficient required to adjust for scaling. This is an

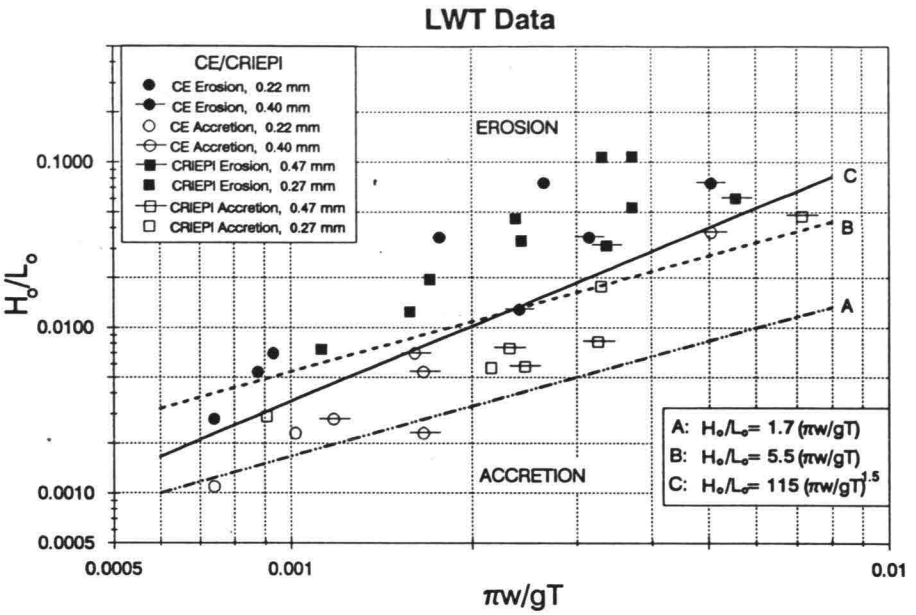


Fig. 8.12. LWT data plotted on the $S_o$ - $G_o$ plane

the magnitude of the empirical coefficient required to adjust for scaling. This is an encouraging result for small-scale model testing.

Because of the relation that exists between $F_o$, $G_o$, and $N_o$, we expect any pair of these parameters will be equally successful in distinguishing erosion and accretion events. This indeed proves to be the case. However, as individual parameters, it is found that $N_o$, $D_o$, and $F_o$ have reasonable capability, but not $G_o$ or $S_o$. The reason inferred for this is that magnitude of wave height and grain size (or fall speed) are leading-order variables controlling whether a beach erodes or accretes, whereas wave period is a secondary variable. Because $S_o$ alone contains no information on grain size, and $G_o$ alone contains no information on wave height, individually they cannot be successful in predicting beach change. For reference, we give the following single-parameter criteria (significant wave height): $F_o = 0.013$; and $D_o = 5{,}000$.

Recently, Dalyrmple (1992) has shown that pairs of parameters $S_o$, $G_o$, $N_o$, $F_o$ can be combined to produce one parameter P, called the "profile parameter," $P = gH_o^2/(w^3T)$. Kraus and Mason (1992) show that $P = 26{,}500$ distinguishes erosion and accretion events in the field, where $H_o$ is significant wave height.

## 8.8 Application: Shallow-Water Linear Mound Design

In this section we consider a calculation procedure for siting of shallow-water linear mounds formed of dredged material. Construction of submerged linear mounds (called "berms" in the dredging literature) can provide an economic alternative for the beneficial use of beach-quality dredged material, keeping it in the littoral zone yet being less expensive than direct placement on the beach in certain situations. The reader can consult McLellan (1990), Hands and Allison (1991), and McLellan and Kraus (1991) for additional information and citations to the literature on this re-activated field involving nearshore placement of sand.

Nearshore berms are submerged, high-relief mounds constructed parallel to shore and composed of clean, predominately beach-quality dredged material. Specifically, the term "berm" refers to a linear feature that resembles a longshore bar, whereas the term "mound" applies to any configuration of artificially placed material.

Nearshore berms are generally divided into two categories, called *feeder berms* and *stable berms*. Feeder berms are constructed of clean sand placed in relatively shallow water to enhance adjacent beaches and nearshore areas by mitigating erosive wave action and by providing additional material for the littoral system. Stable berms are intended to be permanent features constructed in deeper water outside the littoral environment. They may function to attract fish as well as reduce wave energy incident to the coast.

Benefits to the beach are classified as either direct or indirect according to the type of material, berm elevation and length, wave climate, and depth berm placement. The direct benefit is widening of the beach by onshore movement of material from the berm. Indirect benefits are breaking of erosive waves, reduction of storm setup on the beach face, and creation of an artificial storm bar that will reduce erosion by satisfying part of the demand for sediment to be moved offshore during storms. Table 8.1 summarizes associated with the two types of berms.

Table 8.1 Potential Benefits of Nearshore Berms

| | Direct | Indirect | | |
|---|---|---|---|---|
| | Nourish Beach | Attenuate Waves | Reduce Erosion | Stockpile Sand |
| Feeder Berm | Yes | Yes | Yes | No |
| Stable Berm | No | Yes | Yes/No | Yes |

If the placed sediment grain size is compatible with beach samples, a feeder berm can be constructed. If the material is not compatible with the native beach material but does have mounding potential, a stable berm can be considered, whereas it the material is low-density fluid mud, mound construction is unfeasible. Past projects indicate that at least 125 cu m/linear meter are required to build a long feeder berm of significant height (2 to 3 m). Conical-shaped mounds placed in the nearshore focus wave energy behind them and should be avoided. Berm length should be several times the average local wavelength, and the berm should be oriented parallel to the trend of the shoreline to minimize wave focusing and depth limitations of the dredge, and maximize the extent of the shoreline to be protected.

In the following we review the performance of two feeder berm projects conducted by the Corps, one at Gilgo Beach, Long Island, New York, and the other at Silver Strand, California.

### A. Seaward Limit of Littoral Zone

We first calculate the seaward limit of the littoral zone to estimate the depth which would approximately separate successful placement of feeder and stable berms. Of course, for feeder berm design, the shallower the berm is placed the greater the likelihood for material reaching the beach. Eq. 8.33 requires an estimate of the average of the highest waves in 12 hr of a year, which translates to 80 3-hr events in 20 year of Corps of Engineers Wave Information Study (WIS) hindcast summary tables (containing 58,440 wave events at 3-hr intervals). The 12-hr annual average highest wave occurs with a frequency of (80/58440)*100 = 0.14 percent. By inspection of WIS data tables for the respective sites to determine an average wave height corresponding to this percentage, we estimate $H$ = 3.0 m and $T$ = 9 sec for Gilgo, and $H$ = 4.5 m and $T$ = 13 sec for Silver Strand, at the respective hindcast depths of 10 m and 22 m. Shoaling these waves out to deep water and neglecting refraction gives $H_o$ = 3.4 m and $H_o/L_o$ = 0.025 for Gilgo, and 4.7 m and 0.018 for Silver Strand. Substitution of these quantities into Eq. 8.33 yields:

$$h_{sa} = 3.4*(2.3 - 10.9*0.025) = 6.9 \text{ m} = 23 \text{ ft for Gilgo}$$

and

$$h_{sa} = 4.7*(2.3 - 10.9*0.018) = 9.9 \text{ m} = 32 \text{ ft for Silver Strand}$$

From the calculations of $h_{sa}$ it is seen that both berms were placed well inside their respective annual seaward limit of the littoral zone. Accordingly, the berms are expected to function as true feeder berms, providing both the indirect benefits of wave attenuation and reduction of erosional stress, as well as directly nourishing the beach.

## B. Beach Nourishment Potential

To obtain a quantitative estimate of the beach nourishment potential of the two berms under their respective wave environments, wave data in the 20-year average WIS hindcast summary tables were entered in Eq. 8.38 to predict erosional and accretionary conditions. For the two examples, the grain sizes of 0.20 and 0.40 mm were used, yielding fall speeds or 0.025 and 0.053 m/sec at a water temperature of 20° C. Each wave condition was then determined as promoting erosion or accretion.

Interpreted in combination with the frequencies of wave occurrence, of the waves, the calculations provide estimates of frequency of erosion and accretion by cross-shore wave processes. Several observations on the behavior of feeder berms and beach nourishment projects are obtained by this methodology:

1. Accretion is favored for lower wave heights and longer periods, as is evident from the functional dependencies in Eq. 8.38.

2. The longer period waves existing on the west coast tend to promote accretion for episodes of higher waves than is possible on the east coast. Because onshore movement of material in a feeder berm is expected to occur more rapidly under higher waves, this result indicates feeder berms of the same grain size at the same depth will move onshore more rapidly on the west coast than on the east coast.

3. For Gilgo Beach, approximately 40 percent of the waves are accretionary for the 0.20-mm sand. In contrast, the 0.40-mm sand is predicted to experience accretionary conditions more than 75 percent of the time at Gilgo, a strong indication that the material will move into the surf zone and on to the beach.

4. At Silver Strand, the 0.20-mm sand experiences accretion 32 percent of the time from the northern hemisphere sea and swell and 36 percent of the time by the southern hemisphere swell. Although the northern and southern hemisphere wave events are not strictly additive, the relatively high probability for accretion indicates the 0.20-mm sand will move onshore. Table 8.5 also indicates that a berm composed of 0.4-mm sand will have high probability of moving onshore.

By employing any convenient wave breaking criterion involving depth, the approximate frequency of occurrence of erosive waves breaking on the berms can be calculated from knowledge of the berm crest depth.

The above analysis involved cross-shore transport effects. In the overall project design, characteristics of longshore sand transport at the site should also be considered. For example, at Gilgo Beach there is predominant net longshore transport to the west, and a significant portion of the material that moved from the berm is believed to have been transported to beaches down coast. In contrast, at Silver Strand, the net longshore trans-

port is believed to be weak, and most of the berm volume has remained along the profile where it was placed (Andrassy 1991). It is particularly important to consider longshore sand transport if the possibility exists for the material to enter a navigation channel or inlet.

## 8.9 Concluding Discussion

This chapter has considered engineering approaches and applications to cross-shore sediment transport processes and beach profile change. At present, approaches that isolate cross-shore and longshore processes are highly fruitful and appropriate owing to our limited understanding of nearshore hydrodynamics and sediment transport. Ultimately, the nearshore must be treated through a fully three-dimensional model.

Similarly, the material contained in this chapter primarily takes a macroscale of geomorphic approach in describing processes over long spatial scales and in the steady state. As knowledge is gained of the basic physical processes, microscale approaches that are being undertaken now will become more competitive in predictive capability and reliability. Many advances are expected in the coming decade through comprehensive field experiments, laboratory experiments, and the need for coastal engineering to meet the challenge of society to preserve the coast and human life and resources located on the coast.

## Acknowledgements

This work was performed as part of the activities of the Beach Fill Engineering work unit, Shore Protection and Restoration Program, U.S. Army Corps of Engineers. Mses. Marsha W. Darnell and Holley Messing, Coastal Engineering Research Center, assisted in preparing the manuscript. Permission was granted by the Chief of Engineers to publish this information.

## References

Andrassy, C. J. 1991. Monitoring of a nearshore disposal mound at Silver Strand State Park, *Proc. Coastal Sediments '91*, ASCE, 1970-1984.

Bagnold, R. A. 1963. Mechanics of marine sedimentation, *The Sea* (ed. by M. N. Hill), 3, Interscience, New York, 507-528.

Birkemeier, W. A. 1985. Field data on seaward limit of profile change, *J. Waterway, Port, Coastal and Ocean Engrg.*, Vol. 111, No. 3, 598-602.

Bowen, A. J. 1980. Simple models of nearshore sedimentation, beach profiles and longshore bars, *The Coast of Canada* (ed. by S. B. McCann), Geological Survey of Canada, 1-11.

Bruun, P. 1954. Coast erosion and the development of beach profiles. Tech. Memo. No. 44, Beach Erosion Board, U.S. Army Engr. Waterways Expt. Stn., Vicksburg, MS.

Dally, W. R., Dean, R. G., and Dalrymple, R. A. 1985. Wave height variation across beaches of arbitrary profile, *J. Geophys. Res.*, Vol. 90, No. C6, 11917-11927.

Dalrymple, R. A. 1992. Prediction of storm/normal beach profiles, *J. Waterway, Port, Coastal and Ocean Engrg.*, ASCE, Vol. 118, No. 2, 193-200.

Dean, R. G. 1973. Heuristic model of sand transport in the surf zone, *Proc. Engineering Dynamics in the Surf Zone*, Inst. Engineers, Australia, 208-214.

Dean, R. G. 1976. Beach erosion: causes, processes, and remedial measures, *CRC Reviews in Environmental Control*, CRC Press Inc., Vol 6, Is. 3, 259-296.

Dean, R. G. 1977. Equilibrium beach profiles - U.S. Atlantic and Gulf Coasts, Ocean Eng. Rep., 12, Univ. Delaware, 1-45.

Dean, R. G. 1984. Applications of equilibrium beach profile concepts, *Coastal Engineering Abstracts*, ASCE, 140-141.

Dean, R. G. 1987. Coastal sediment processes: toward engineering solutions, *Proc. Coastal Sediments '87*, ASCE, 1-24.

Dean, R. G. 1991. Equilibrium beach profiles: characteristics and applications, *Journal of Coastal Res.*, 7(1), 53-84.

Dean, R. G. and Maurmeyer, E. M. 1983. Models for beach profile response, In: Komar, P. D. (Ed.), *CRC Handbook of Coastal Process and Erosion*, CRC Press, Boca Raton, FL, 151-166.

Hallermeier, R. J. 1979. Uses for a calculated limit depth to beach erosion, *Proc. 16th Coastal Engineering Conf.*, ASCE, 1493-1512.

Hallermeier, R. J. 1981a. A profile zonation for seasonal sand beaches from wave climate, *Coastal Eng.*, 4, 253-277.

Hallermeier, R. J. 1981b. Terminal settling velocity of commonly occurring sand grains, *Sedimentology*, 28(6), 859-865.

Hallermeier, R. J. 1983. Sand transport limits in coastal structure designs, *Proc. Coastal Structures '83*, ASCE, 703-716.

Hands, E. B. 1976. Observations of barred coastal profiles under the influence of rising water levels, Eastern Lake Michigan, 1967-71, Tech. Rep. 76-1, Coastal Eng. Res. Center, U.S. Army Engr. Waterways Expt. Stn., Vicksburg, MS.

Hands, E. B. and Allison, M. C. 1991. Mound migration in deeper water and methods of categorizing active and stable depths, *Proc. Coastal Sediments '91*, ASCE, 1985-1999.

Hanson, H., and Kraus, N. C. 1989. GENESIS: generalized model for simulating shoreline change; Report 1, technical reference. Tech. Rep. CERC-89-19, U.S. Army Engr. Waterways Expt. Stn., Coastal Engrg. Res. Center, Vicksburg, MS.

Hayes, M. O., and Boothroyd, J. C. 1969. Storms as modifying agents in the coastal environment, *Coastal Environments, Northeast Massachusetts and New Hampshire*, Eastern Section, Soc. of Econom. Paleontologists and Mineralogists, Field Guide. Reprinted in Davis, R. A. ed., 1987, *Beach and Nearshore Sediments and Processes*, SEPM Reprint Series Number 12, SEPM Tulsa, OK, 25-39.

Howd, P. A. and Birkemeier, W. A. 1987. Storm-induced morphology changes during DUCK85, *Coastal Sediments '87*, ASCE, 834-847.

Hughes, S. A. and Fowler, J. E. 1990. Midscale physical model validation for scour at coastal structures, Tech. Rep. CERC-90-8, U.S. Army Engr. Waterways Expt. Station, Coastal Engrg. Res. Center, Vicksburg, MS.

Iwagaki, Y. and Noda, H. 1963. Laboratory studies of scale effects in two-dimensional beach processes, *Proc. 8th Coastal Engineering Conf.*, ASCE, 194-210.

Johnson, J. W. 1949. Scale effects in hydraulic models involving wave motion, *Trans. Amer. Geophys. Union*, 30(4), 517-525.

Kajima, R., Shimizu, T., Maruyama, K., and Saito, S. 1983. Experiments of beach profile change with a large wave flume, *Proc. 18th Coastal Engineering Conf.*, ASCE, 1385-1404.

Keulegan, G. H. 1945. Depths of offshore bars, Eng. Notes No. 8, Beach Erosion Board, U.S. Army Engr. Waterways Expt. Station, Vicksburg, MS.

Keulegan, G. H. 1948. An experimental study of submarine sand bars, Tech. Rep. No. 3, Beach Erosion Board, U.S. Army Engr. Waterways Expt. Station, Vicksburg, MS.

Kraus, N. C. and Harikai, S. 1983. Numerical model of the shoreline change at Oarai Beach, *Coastal Eng.*, 7(1), 1-28.

Kraus, N. C. and Larson, M. 1988. Prediction of initial profile adjustment of nourished beaches to wave action, *Proc. Beach Preservation Technology '88*, Florida Shore and Beach Preservation Association, Inc., 125-137.

Kraus, N. C., Larson, M. and Kriebel, D. L. 1991. Evaluation of beach erosion and accretion predictors, *Proc. Coastal Sediments '91*, ASCE, 572-587.

Kraus, N. C. and Mason, J. M. 1992. Discussion of prediction of storm/normal beach profiles, *J. Waterway, Port, Coastal and Ocean Engrg.*, submitted.

Kraus, N. C., Smith, J. M., and Sollitt, C. K. 1992. SUPERTANK laboratory data collection project, *Proc. 23rd Coastal Engrg. Conf.*, ASCE, in press.

Kriebel, D. L. 1987. Beach recovery following Hurricane Elena, *Proc. Coastal Sediments '87*, ASCE, 990-1005.

Kriebel, D. L. and Dean, R. G. 1985. Numerical simulation of time-dependent beach and dune erosion, *Coastal Engrg.*, Vol 9, 221-245.

Kriebel, D. L., Kraus, N. C. and Larson, M. 1991. Engineering methods for predicting beach profile response, *Proc. Coastal Sediments '91*, ASCE, 557-571.

Larson, M., and Kraus, N. C. 1989a. SBEACH: numerical model for simulating storm-induced beach change; Report 1, empirical foundation and model development. Tech. Rep. CERC-89-9. Coastal Engrg. Res. Center, U.S. Army Engr. Waterways Expt. Stn., Vicksburg, MS.

Larson, M. and Kraus, N. C. 1989b. Prediction of beach fill response to varying waves and water level, *Proc. Coastal Zone '89*, ASCE, 607-621.

McLellan, T. N. 1990. Nearshore mound construction using dredged material, *J. Coastal Research*, Special Issue No. 7, 99-107.

McLellan, T. N. and Kraus, N. C. 1991. Design guidance for nearshore berm construction, *Proc. Coastal Sediments '91*, ASCE, 2000-2011.

Moore, B. D. 1982. Beach profile evolution in response to changes in water level and wave height, unpublished M.S. thesis, U. Delaware, Newark, DE.

Sallenger, A. H., Jr., Holman, R. A. and Birkemeier, W. A. 1985. Storm-induced response of a nearshore bar system, *Marine Geol.*, 64, 237-257.

Saville, T., Jr. 1957. Scale effects in two-dimensional beach studies, *Proc. 7th General Meeting Int. Assoc. Hydraulic Res.*, A3.1-A3.8.

Shepard, F. P. and Inman, D. L. 1950. Nearshore circulation related to bottom topography and wave refraction, *Trans. Am. Geophys. Union*, 31(4), 555-556.

Sonu, C. J. 1970. Beach changers by extraordinary waves caused by hurricane Camille, Coastal Studies Inst., Tech. Rep. 77, Louisiana State Univ., Baton Rouge, LA, 33-45.

Sunamura, T. 1989. Sandy beach morphology elucidated by laboratory modeling, in V. C. Lakhan and A. S. Trenhale (eds.), *Applications in Coastal Modeling*, Elsevier, New York, 159-213.

Sunamura, T. and Maruyama, K. 1987. Wave-induced geomorphic response of eroding beaches - with special reference to seaward migrating bars - , *Proc. Coastal Sediments '87*, ASCE, 788-801.

Zenkovich, V. P. 1967. Submarine sand bars and related formations, In: *Processes of Coastal Development*, ed. J. A. Steers, Oliver and Boyd Ltd, New York, NY, 219-236.